

Statistical procedures for developing earthquake damage fragility curves

David Lallemand^{*,†}, Anne Kiremidjian and Henry Burton

Department of Civil and Environmental Engineering, Stanford University, Stanford, CA, 94305, USA

SUMMARY

This paper describes statistical procedures for developing earthquake damage fragility functions. Although fragility curves abound in earthquake engineering and risk assessment literature, the focus has generally been on the methods for obtaining the damage data (i.e., the analysis of structures), and little emphasis is placed on the process for fitting fragility curves to this data. This paper provides a synthesis of the most commonly used methods for fitting fragility curves and highlights some of their significant limitations. More novel methods are described for parametric fragility curve development (generalized linear models and cumulative link models) and non-parametric curves (generalized additive model and Gaussian kernel smoothing). An extensive discussion of the advantages and disadvantages of each method is provided, as well as examples using both empirical and analytical data. The paper further proposes methods for treating the uncertainty in intensity measure, an issue common with empirical data. Finally, the paper describes approaches for choosing among various fragility models, based on an evaluation of prediction error for a user-defined loss function. Copyright © 2015 John Wiley & Sons, Ltd.

Received 10 September 2013; Revised 21 October 2014; Accepted 23 October 2014

KEY WORDS: fragility curves; maximum likelihood estimation; generalized linear model; generalized additive model; kernel smoothing

1. INTRODUCTION

Earthquake damage to ground motion relationships is a key component for earthquake loss estimation and the performance-based analysis of the risk of structures. Also called fragility curves, they describe the probability of experiencing or exceeding a particular level of damage as a function of ground-shaking intensity. Depending on the source of data used to develop these relationships, they can be categorized as (i) empirical fragility curves, based on post-earthquake damage evaluation data [1–4]; (ii) analytical fragility curves, based on structural modeling and response simulations [5–8]; or (iii) heuristic fragility curves, based on expert opinion [9, 10]. The resulting fragility relationships are represented either in discrete form, known as damage probability matrices [2], or continuous fragility functions.

This study describes several statistical procedures for developing continuous earthquake damage fragility functions. Both empirical and analytical data are used to demonstrate the methods. The fragility curves describe the probability of exceeding a particular damage state as a function of ground motion intensity. Although real data are used, the examples shown are meant only to illustrate options for fitting fragility curves to data, as well as approaches to choosing among them.

^{*}Correspondence to: David Lallemand, Department of Civil and Environmental Engineering, Stanford University, Stanford, CA, 94305, USA.

[†]E-mail: davidcbl@stanford.edu

Two data sets are used in this study. The first consists of field assessments from the main shock of the January 12, 2010 earthquake in Haiti, conducted by the Haitian Ministry of Public Works [11]. Over 47,000 buildings are used in this data set, corresponding to infill frame buildings each categorized within one of the seven damage states following the Applied Technology Council-13 nomenclature [10]: none, slight, light, moderate, heavy, major, and destroyed. These buildings are distributed within nearly 1000 sites, each having 500 m \times 500 m resolution. The ground motion intensity measure (IM) used is the peak ground acceleration (PGA). Because no ground motion recordings were made in Haiti at the time of the earthquake, the ground motion intensity was estimated at each site using the Boore–Atkinson 2008 ground motion prediction equation (GMPE), appropriate for shallow crustal earthquakes in active tectonic regions [12]. The source model for the January 12, 2010 event was produced by the United States Geological Survey [13]. The ground motion intensity at each site is estimated and therefore uncertain. The uncertainty in IM is addressed later in the paper.

For each IM in the database, we can obtain the fraction of buildings exceeding a particular damage state, as shown in Figure 1(a). The size of the dots in the figure corresponds to the number of observations (buildings) at that IM. The fitted fragility curves attempt to predict the probabilities of exceeding a particular damage state in a way that is most consistent with the observed fraction of buildings above that damage state.

The second data set is obtained from the collapse performance assessment of an eight-story infill frame building using the Incremental Dynamic Analysis (IDA) technique [14]. Nonlinear dynamic analyses are conducted on a two-dimensional (planar) model developed in OpenSees [15] using the 22 far-field ground motion set and scaling method outlined in Federal Emergency Management Agency (FEMA) P695 [16]. The first mode spectral acceleration (S_a) is used as the ground motion IM. The overall analysis approach is based on the methodology developed by Burton and Deierlein [17] for simulating seismic collapse in non-ductile reinforced concrete frame buildings with infill. The results from this analytical model take the form of a set S_a values corresponding to onset of collapse (one S_a data point for each ground motion time history). These results are described in Table I for any researcher wanting to reproduce results or test further methods for comparison.

Both data sets are for the collapse damage state, but the methods are applicable for any other damage state. Therefore, any other damage state can be substituted for the collapse and used in the development of the fragility functions presented in this paper. The fragility functions for damage states other than collapse, however, will represent the probability of being or exceeding that damage state as a function of the ground motion.

2. LOGNORMAL CDF FRAGILITY CURVE

The lognormal CDF has often been used to model earthquake damage fragility (Equation 1). It is a simple parametric model, which historically has been found to provide good representation of

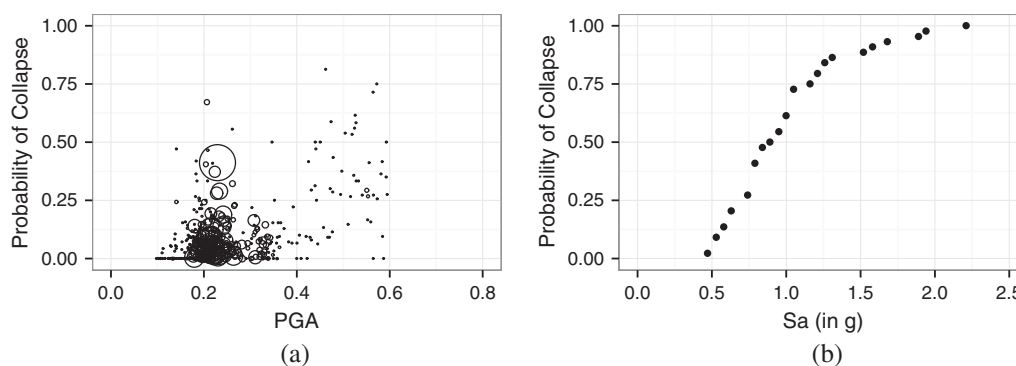


Figure 1. Damage data used for fitting fragility models: (a) real data from the 2010 Haiti earthquake (the size of points reflects the number of buildings at that IM level and (b) incremental dynamic analysis results for an eight-story building.

Table I. Analytical data from incremental dynamic analysis of an eight-story concrete frame building with infill.

Ground motion	1	2	3	4	5	6	7	8	9	10	11
Sa at collapse	0.53	0.58	1.00	1.00	0.79	0.79	0.74	0.47	1.05	0.53	0.79
Ground motion	12	13	14	15	16	17	18	19	20	21	22
Sa at collapse	1.16	1.05	1.21	0.79	1.05	1.00	0.63	2.21	1.26	0.63	0.89
Ground motion	23	24	25	26	27	28	29	30	31	32	33
Sa at collapse	1.58	0.79	0.53	0.95	1.94	0.63	1.21	0.79	0.74	0.84	0.84
Ground motion	34	35	36	37	38	39	40	41	42	43	44
Sa at collapse	0.95	0.74	1.31	1.89	1.05	1.52	1.05	0.58	1.26	0.84	1.68

Sa, spectral acceleration.

earthquake damage fragility [5, 7, 18–20], and has significant precedent for seismic risk modeling [21–23]. The lognormal cumulative distribution further has numerous convenient characteristics for modeling fragility. As is the case with any CDF, it is bounded between 0 and 1 on the y-axis, satisfying the constraint that the probability of collapse (or any other damage state) is likewise bounded between 0 and 1. It has a lower bound of 0 on the x-axis, which satisfies the expectation of non-negative IMs and of no damage at an IM of 0. It also has the mathematical convenience that when a lognormally distributed random variable is multiplied or divided by factors (factors of safety for instance), which are themselves uncertain and lognormally distributed, the resulting fragility curve is still lognormally distributed [24]. This characteristic of multiplicative reproducibility of the lognormal distribution has made it a powerful tool for developing code-oriented reliability metrics, including nuclear power plant design [25].

2.1. Lognormal CDF fit by method-of-moments (MM)

When the IM at the damage threshold of interest (e.g., collapse) is known for all data points, the MM can be used to obtain the parameters of the lognormal distribution, which matches the moments of the data sample. This type of data is only available when conducting IDA or when testing experimental samples until failure. In particular, the MM is often used in IDA [14]. In this approach, a suite of ground motion time histories are used to analyze the structural response of a building. The ground motion time histories are scaled until the threshold of interest (e.g., collapse) is reached for all ground motions. Table I shows the results from this type of analysis, where 44 earthquake time histories were scaled until collapse of the analytical building model. The logarithmic moments of the distribution of Sa at collapse are then easily computed, and the resulting collapse fragility curve is described by the following lognormal CDF curve:

$$P(C|IM = IM_i) = \Phi\left(\frac{\ln(IM_i) - \bar{\mu}}{\bar{\beta}}\right) \tag{1}$$

where Φ is the standard cumulative normal distribution function, and the sample mean and standard deviation are calculated as $\bar{\mu} = E[\ln(IM_{collapse})]$ and $\bar{\beta} = \sqrt{Var(\ln(IM_{collapse}))}$.

This same procedure can also be used for experimental data if all specimens are tested until failure (or other threshold) [26]. It is indeed noted that the MM approach can be used only for limited types of data. It cannot be used for empirical data nor for truncated IDA (where a limit is imposed on the scaling of ground motions) or multiple stripes analysis (where dynamic analysis is conducted only for a few IMs) [27].

2.2. Lognormal CDF fit by minimizing weighted sum of squared error (SSE)

Least squares regression is an alternative approach to estimate the parameters of the fragility curve without directly calculating the sample moments. It can therefore be used both for analytical data and post-earthquake damage results. This approach determines the $\hat{\mu}$ and $\hat{\beta}$ parameter estimates that minimize the SSE between the probabilities predicted by the fragility function and the fractions observed from the data [27, 28]. The errors can further be weighted by the number of observed data at each IM level (or other weights reflecting the uncertainty of each data point). Weighted least

squares regression is indeed a common method to treat heteroscedastic data, where data points have different levels of uncertainty. Conducting weighted least squares regression allows for the larger points in Figure 1(a) to have greater influence on the resulting curve, because they represent more buildings. In this approach, a lognormal CDF can be fitted to the damage data using parameters estimated from the following weighted least-squared optimization procedure:

$$\hat{\mu}, \hat{\beta} = \arg \min_{\mu, \beta} \sum_{i=1} N_i \left(\frac{n_i}{N_i} - \Phi \left(\frac{\ln(IM_i) - \mu}{\beta} \right) \right)^2 \quad (2)$$

where n_i/N_i is the observed ratio of collapsed buildings at $IM = IM_i$.

This approach can be used to fit functions of forms other than lognormal CDF curves.

2.3. Lognormal CDF fit by maximum likelihood estimation (MLE)

Like the SSE method, the MLE method can be used for both analytical and post-earthquake damage results. Previous studies have demonstrated the use of MLE for earthquake fragility modeling of buildings and bridges [24, 27, 28]. The concept of the MLE method is to estimate the parameters of the distribution that maximize the probability of occurrence of the observed data.

Given a set of post-earthquake damage data for instance, the probability of having n_i collapsed buildings out of N_i total buildings at a ground motion intensity $IM = IM_i$ can be represented by the binomial distribution

$$P(n_i \text{ in } N_i \text{ collapse} | IM = IM_i) = \binom{N_i}{n_i} p_i^{n_i} (1 - p_i)^{N_i - n_i} \quad (3)$$

where p_i is the probability of collapse at $IM = IM_i$.

Following the MLE method, the goal is to obtain the function for p that maximizes the likelihood of observing all the (n_i, N_i) pairs. This is therefore obtained by maximizing the 'likelihood function', equal to the product of the binomial probabilities for each IM in the database.

$$\text{Likelihood} = \prod_{i=1}^m P(n_i \text{ in } N_i \text{ collapse} | IM = IM_i) = \prod_{i=1}^m \binom{N_i}{n_i} p_i^{n_i} (1 - p_i)^{N_i - n_i} \quad (4)$$

For a fragility function following the form of a lognormal CDF, p_i is replaced by the equation of the lognormal CDF, and the parameter estimates $\hat{\mu}$ and $\hat{\beta}$ (logarithmic mean and standard deviation) of the lognormal CDF are estimated such that they maximize the likelihood function. It should be noted that any other functional form can be substituted for p_i if preferred to the lognormal CDF. Replacing p by the equation of the binomial distribution, the parameters are estimated by maximizing the logarithm of the likelihood, which is equivalent and computationally more efficient than maximizing the likelihood function itself

$$\hat{\mu}, \hat{\beta} = \arg \max_{\mu, \beta} \sum_{i=1} \left[n_i \ln \left(\Phi \left(\frac{\ln(IM_i) - \mu}{\beta} \right) \right) + (N_i - n_i) \ln \left(1 - \Phi \left(\frac{\ln(IM_i) - \mu}{\beta} \right) \right) \right] \quad (5)$$

where $\hat{\mu}$ and $\hat{\beta}$ are the estimates of μ and β , and the $\ln \binom{N_i}{n_i}$ term has been removed because it is a constant, therefore having no impact on the maximization.

Standard software packages such as Microsoft Excel, MATLAB, or R can be used to obtain the parameters $\hat{\mu}$ and $\hat{\beta}$ that maximize Equation 5. These parameters are used in Equation 1 to obtain the fitted lognormal CDF fragility function.

Although simplest to implement given the required data, the MM often provides poor fit to data. As seen in Figure 2(b), it underestimates the probability of collapse for most IMs. This is a typical finding, because the MM simply matches the central distribution characteristics (median and variance) rather than the entire distribution.

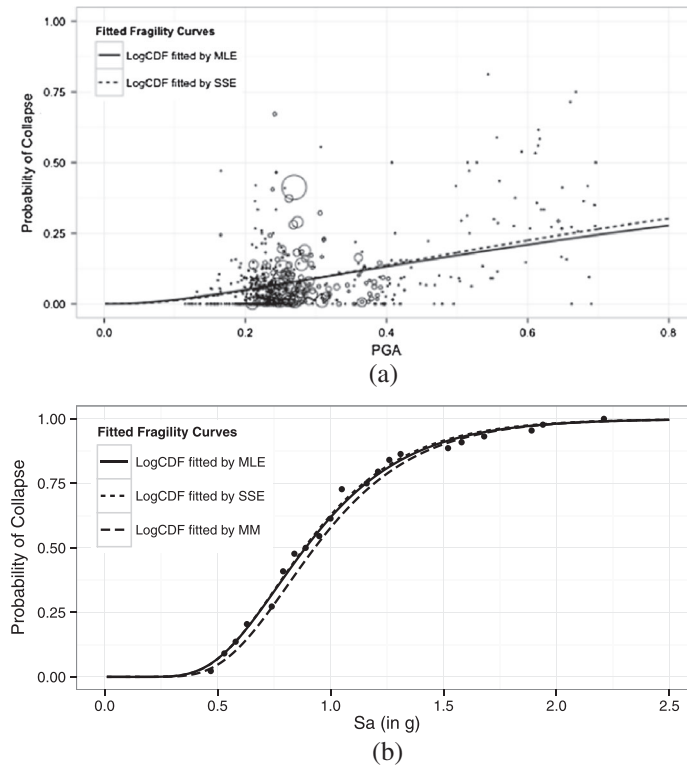


Figure 2. Lognormal CDF fragility curves fitted to with MM, MLE, and SSE optimization to (a) Haiti damage survey data and (b) analytical IDA results.

2.4. MM, SSE, and MLE compared

The SSE method is simple to implement and as seen in Figure 2 can often provide very similar results to those obtained from MLE. Implicit, however, in a model that minimizes least-squared error is that the error in the prediction is normally distributed, and the variance in the error is independent of the prediction. This is clearly not the case for damage data, which are binomially distributed when using exceedance/non-exceedance data or bounded between 0 and 1 when using damage fraction data. The assumption of independent error variance can further result in poor fit at the low and high portions of the curve. For example, in the SSE approach and a given fragility curve, a 10% error on a true probability of 15% has equal influence on the estimator as the same 10% error on a true probability of 50%. MLE does not have this limitation, as it is solved by iterative re-weighted least squares, where each weight is inversely proportional to the variance of the binomial distribution centered at the predicted response. In the MLE method, because the damage data are binomially distributed (i.e., collapse or not collapse), the least squares optimization is weighted based on the variance equal to $m(1 - m)$, where m is the mean of the binomial distribution, which is also the predicted response. For a low or high mean m , the variance is therefore small, and the residuals are weighted accordingly. Therefore, the MLE-based lognormal CDF fragility curve is preferable to both the MM-based and SSE-based lognormal CDF curves.

3. GENERALIZED LINEAR MODELS (GLMS)

Generalized linear models are commonly used for regression analysis of dichotomous data (zeros and ones, such as collapsed or non-collapsed structures). GLMs are a variation of ordinary linear regression, in which the predictor variables are linearly related to the response via a link function. The GLM is made up of three parts: (i) a conditional probability distribution of the exponential

family; (ii) a linear predictor; and (iii) a link function, through which the linear predictor is related to the response [30]. GLM models can be written as follows:

$$g(\mu) = \eta = \alpha + \beta_1 X_1 + \beta_2 X_2 + \dots + \beta_n X_n \quad (6)$$

where μ is the expected response given predictor variables X_1, X_2, \dots, X_n . The term η is the linear predictor, which is related to the expected response through the link function $g(\cdot)$.

For developing fragility curves, Equation 6 reduces to a single independent variable (typically, the logarithm of IM) and two linear coefficients (intercept α and a single coefficient β), and μ is the expected probability exceeding a particular damage state (DS) threshold

$$P(DS \geq ds | IM) = g^{-1}(\alpha + \beta \log(IM)) \quad (7)$$

The process of fitting a GLM then involves finding the coefficients that maximize the likelihood function based on assumptions of a conditional distribution of the exponential family. In the case of fragility, the binomial distribution is the most natural choice.

One advantage of GLMs is that they all use MLE for fitting the model. The MLE is found by solving the score function by means of iteratively re-weighted least squares, which as described earlier provide weights on the error that are inversely proportional to the conditional variance. This solves the issue of non-independent conditional variance. In this section, we describe GLMs for fitting fragility curves using the probit and logit link functions, which are the most commonly used for dichotomous response data. We also explore two assumptions on the conditional distribution (binomial and Gaussian).

3.1. Probit GLM model with binomial distribution and log input variable (IM)

An exactly equivalent result to fitting a lognormal CDF by MLE (as described in Section 2) can be obtained by fitting a GLM assuming a binomial response and using a probit link function with the logarithm of the predictor variable. This is because the probit model fits a standard normal cumulative distribution, and therefore, a probit model fit to the logarithm of the input variable describes a lognormal cumulative distribution [27, 31]. The optimization of GLMs is furthermore conducted through MLE, and therefore, the models are equivalent. The GLM model takes the form as follows:

$$P(DS \geq ds | IM) = \Phi(\alpha + \beta \log(IM)) \quad (8)$$

This model can therefore be considered simply a different formulation of the MLE-based lognormal CDF curve fitting in Section 2. An advantage to the GLM formulation is that these models are often pre-existing in common software packages (such as R or MATLAB), which automatically also compute useful outputs for evaluating goodness of fit (Akaike information criteria, R-squared measure, etc.) and confidence on the estimates.

3.2. Logistic GLM model with log input variable

This model is a GLM assuming binomial response distribution and using a logit link function, once again with logarithm of the IM. This is 'logistic regression' with log-transformed predictor variables. It is noted that logistic regression has previously been used for fragility modeling [32, 33]. The logit link is often used for dichotomous data (in 'logistic regression') and is the canonical link for the binomial distribution [30]. In practice, the logit and probit models result in very similar curves, although the probit model tends to have sharper increase at low IMs and sharper flattening at high IMs. One advantage of logistic regression is that results are easy to interpret. The estimated β coefficient obtained from logistic regression is equal to the increase in log odds of the response (i.e., odds of collapse) due to a unit increase in the independent variable (i.e., $\log(IM)$).

In addition to the probit and logit link functions for binomial data, the complementary log–log (commonly known as ‘clog-log’) link can also be used.

4. GENERALIZED ADDITIVE MODELS (GAM)

Generalized additive models are an extension of GLMs in which the requirement of linear combination of parameters is relaxed. They are often used to identify non-linear effects. These methods are more complex and require more background but can often provide very good results [34, 35]. GAM models were recently introduced for modeling earthquake fragility by Rosetto *et al.* [36]. Recalling that generalized *linear* models relate the mean response to predictors through a linear regression model and a link function, generalized *additive* models simply replace the linear coefficients with unspecified smoothing functions

$$g(\mu) = \eta = \alpha + f_1X_1 + f_2X_2 + \dots + f_nX_n \tag{9}$$

where f_1, f_2, \dots, f_n are non-parametric scatterplot smoothers, usually cubic smoothing splines. These splines fit cubic polynomial curves within sections, connected at points (called *knots*), creating a continuous curve. The general effect of the smoothers is to relax the constraints of the standard GLM models. During the fitting process for additive models, a smoothing parameter λ can be specified.

Generalized additive models are semi-parametric and therefore cannot be summarized by linear coefficient parameters and a link function. Compared with GLM models, GAM models are more flexible and provide very good fit to data when significant nonlinearities in predictor variables are present. The smoothing parameter is used to balance between bias and variance (over-smoothing and over-fitting), as seen in Figure 3. An infinite smoother reduces to a GLM.

5. GAUSSIAN KERNEL SMOOTHING (GKS)

Gaussian kernel smoothing is a non-parametric regression method that helps to smoothen otherwise erratic data and can be used to develop non-parametric fragility functions [37, 38]. It uses a kernel, which for each data assigns a weight that is inversely related to the distance between the data value and the input of the fragility function of interest. In GKS, the weights are equal to the evaluation at all data points of the Gaussian density distribution centered at the IM value of interest and with variance chosen depending on the smoothing requirements. The probability of exceeding damage state ds given $IM = im_i$ can therefore be computed as follows:

$$P(DS \geq ds | IM = im_i) = \frac{\sum_{p=1}^n I(ds_p \geq ds) \times \Phi^{-1}\left(\frac{im_i - im_p}{h}\right)}{\sum_{p=1}^n \Phi^{-1}\left(\frac{im_i - im_p}{h}\right)} \tag{10}$$

where $I(ds_p \geq ds)$ is the indicator function, equal to 1 for $ds_p \geq ds$ and 0 otherwise, h is the kernel bandwidth (standard deviation of the Gaussian kernel), subscript p refers to observed data, and subscript i refers to the IM level of interest (Figure 3).

Gaussian kernel smoothing has the advantage of avoiding any assumption on the shape of the fragility function. Because the fragility curve is no longer constrained to a particular functional shape, it will tend to more closely fit the data, with the possible danger of over-fitting. The kernel bandwidth is used to balance between variance (over-fitting) and bias (over-smoothing), as demonstrated in Figure 4(a). GKS can also be conducted on the logarithm of IM, often producing better results.

A common issue with kernel weighted-based smoothing is that the resulting functions exhibit bias at the boundaries of the domain, because the kernel becomes asymmetric at the boundary (data exist only on one side of the kernel). The issue of localized bias at the boundary results in non-zero probabilities

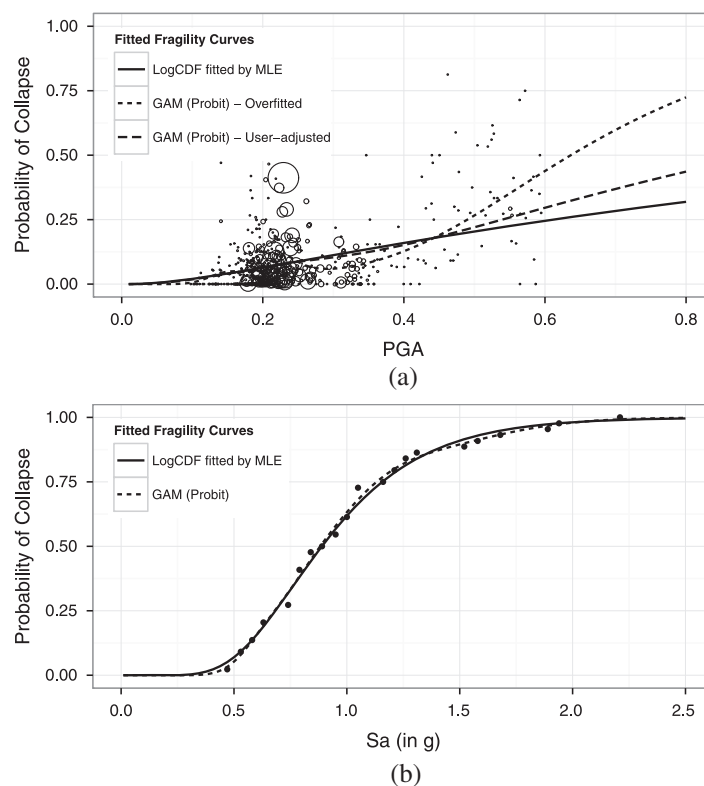


Figure 3. Generalized additive model-based fragility curve with probit link function, binomial distribution, and logarithmic IM variables and lognormal CDF fragility fitted with MLE for (a) Haiti damage survey data and (b) analytical IDA results.

of damage at zero IM intensity as shown in Figure 4(b), which clearly does not reflect underlying physical constraints. It can therefore be forced to zero through zero-padding at the boundary. This process simply adds artificial values of zero at the zero IM level. Because of the kernel weighting of every data point, the effect of zero-padding is localized. Another approach to address the localized bias is through kernel-weighted local linear regression. This method fits straight lines rather than constants locally. Finally, it is noted that GKS can also be used to develop conditional probabilities of collapse given IM, through two-dimensional GKS [38]. The development and application of kernel-weighted linear regression and two-dimensional kernel smoothing used in fragility modeling is described by Noh *et al.* [38].

6. CUMULATIVE LINK MODELS FOR ORDINAL DAMAGE STATES

All models described previously treat damage data as nominal (i.e., that damage states are unrelated). However, one useful characteristic of damage state data is that it can be ordered (no damage, slight damage, moderate damage, etc.) even though the 'distances' between damage categories are unknown (is slight damage half as much as moderate damage?). These data are therefore an example of ordinal data, as opposed to nominal data, where data categories are assumed to have no relation other than being mutually exclusive. The ordinality of variables can be used to develop fragility curves for all damage states simultaneously using cumulative link models. These models further take advantage of the ordinal characteristics of data to improve the parsimony and power of models [31]. They ensure the proper treatment of cumulative damage probabilities (fragility curves will never cross) and take advantage of data from all damage states to create fragility curves for each individual damage state.

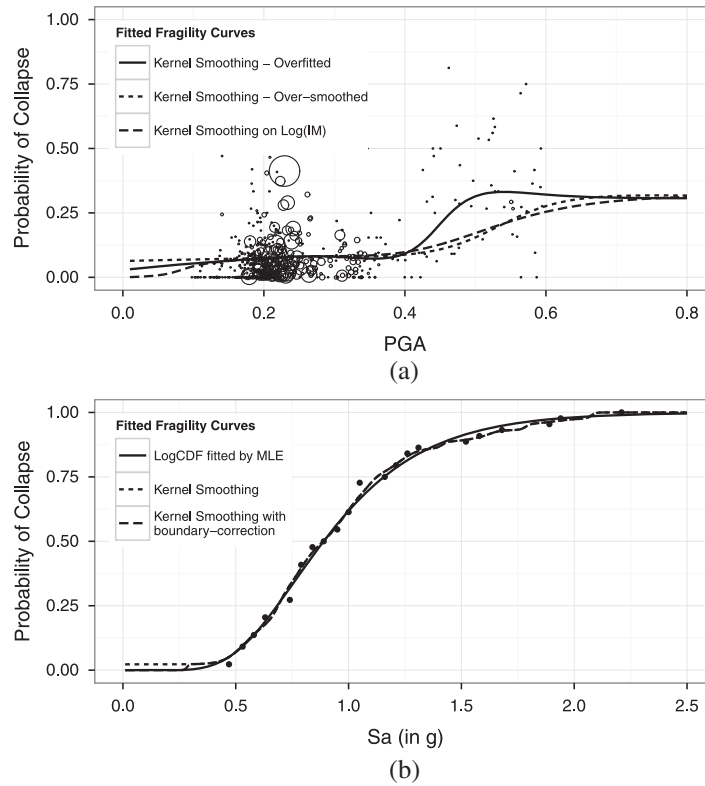


Figure 4. Gaussian kernel smoothing non-parametric fragility curves and lognormal CDF fragility fitted with MLE for (a) Haiti damage survey data and (b) analytical IDA results.

Cumulative link models are an extension of GLMs described in Section 3, applied to ordinal data. For earthquake fragility modeling, the damage state ordering forms cumulative probabilities for each damage state j

$$P(DS \geq DS_j | IM) = g^{-1}(a_j + \beta \log(IM)), \quad j = 1, \dots, j - 1 \tag{11}$$

Each cumulative probability has its own intercept a_j but shares the same effect β . This common effect β is justified when considering that discrete ordinal damage states are coarsened versions of an underlying continuous latent variable of damage [31]. Common link functions used are the logit

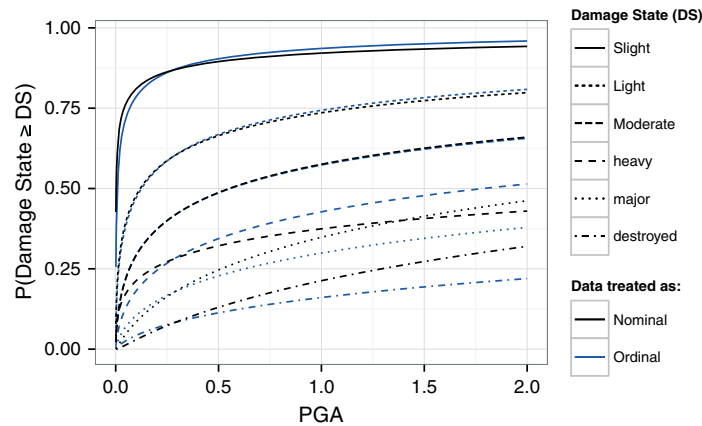


Figure 5. Fragility curves for all damage state fit with a cumulative probit model (blue) and individual probit GLMs (black).

and probit link functions, resulting in the proportional odds model and ordered probit model, respectively. As in the GLM models, using the probit link in Equation 11 fits MLE-based lognormal CDF fragility curves.

Although the common effect β leads to simpler models and therefore less flexibility (fewer parameters), the cumulative link models have two significant advantages. First, cumulative link models never violate the proper ordering among cumulative probabilities. This addresses the issue of ‘crossing fragility curves’, which often arise when treating the data as nominal [39]. This is exemplified when fitting fragility curves to the Haiti data shown in Figure 5. Second, cumulative link models are particularly useful for developing fragility curves when data for a specific damage state are sparse. This is because all damage data (for all damage states) are used for each fragility curve. Hence, even when very few collapses are observed, the model uses information from other damage states to inform and estimate a collapse fragility curve, consistent with cumulative damage state probabilities. In fact, this is very common, as there is usually little data on extreme damages in empirical data sets.

7. BAYESIAN METHODS

In addition to the methods described here, Bayesian methods can be used to update fragility curves based on new data. Typically, analytical or expert-based fragility curves can be updated based on new data including field-based damage data or experimental testing results. This poses advantages when empirical data only cover a small range of IMs or in order to refine general (non-geographically specific) fragility curves for local building vulnerability. Such methods are described in several other references [40–42].

8. UNCERTAINTY IN INTENSITY MEASURE

Uncertainty in IM is a common issue for the development of empirical fragility curves. Indeed, for most empirical damage data, the ground motion is not measured at each site but rather inferred based on GMPE or a combination of recordings and GMPE-based inferences. Modern GMPEs typically take the form

$$\begin{aligned} \ln(IM) &= f(M, R, Vs30) + \varepsilon_1\sigma + \varepsilon_2\tau \\ \ln(IM) &= \ln(\overline{IM}) + \varepsilon_1\sigma + \varepsilon_2\tau \end{aligned} \quad (12)$$

where σ and τ are period dependents and reflect the intra-event (within event) and inter-event (event-to-event) uncertainties, respectively.

The combined uncertainty $\sigma_T = \sqrt{\sigma^2 + \tau^2}$ can be significant. For example, the logarithmic uncertainty is typically around 0.5 for PGA. This leads to issues when performing a regression, because the explanatory variable (IM) is not observed but estimated. In fact, such error usually leads to the attenuation of estimated effect (near-systematic negative bias in the effect estimator) [43]. This is demonstrated in the following text and shown in Figure 7.

Ideally, it would be possible to develop an ‘error-in-variables’ model (also known as ‘measurement error model’) for fragility curves based on inferred ground motion IMs. Most such models require a so-called ‘instrumental variable’, which is correlated with the true IM but not correlated with its measurement error. In practice, such instrumental variable rarely exists, although perhaps modified Mercalli intensity measured through United States Geological Survey (USGS’s) ‘did-you-feel-it’ platform could be investigated. In addition, measurement error models require that the measurement error in the independent variable be independent from the true variable (classical error) and mean zero. The first condition can be met when regressing on the logarithmic IM (classical error shown in Equation 12). However, by definition, the event-to-event term $\varepsilon\tau$ in Equation 12 is perfectly correlated for any given data set from a single earthquake. Furthermore, the intra-event term $\varepsilon\sigma$ is

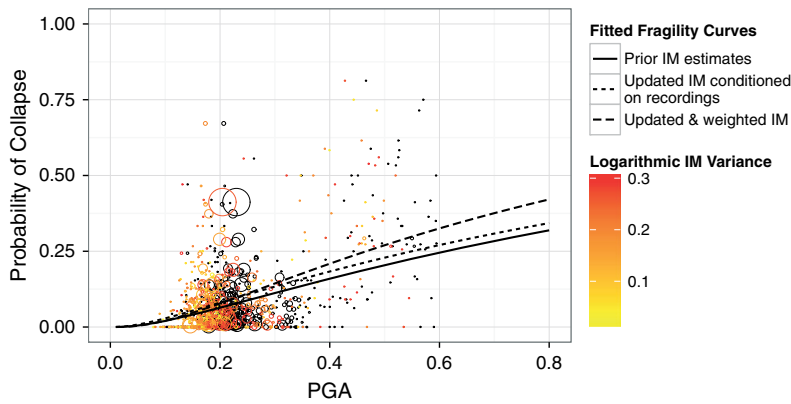


Figure 6. Fragility curves updated by conditioning ground motion intensity fields to known intensity measure at recording stations and weighted inversely to the variance of intensity measure.

spatially correlated, so it is possible for a significant portion of damage observations (possibly all) to be at sites with correlated intensity. Both facts lead to violation of the mean zero measurement error requirement for measurement–error regression models.

Therefore, the only clear approach to reducing the bias introduced by uncertainty in the IM is to reduce this uncertainty. This is possible if ground motion recordings are available. Even a single recording can be used to update expected IM at all sites, as well as reduce the inter-event uncertainty. Because ground motions are spatially correlated, the intra-event uncertainty can also be reduced in the region within the correlation distance of the recording.

This is demonstrated using the Haiti data. One million spatially correlated ground motion fields are produced using the Boore–Atkinson 2008 GMPE [12] and the spatial correlation model for PGA developed by Jayaram and Baker [44]. Without any other constraint, the median and logarithmic standard deviation of the one million spatially correlated IM simulations at each site match those obtained from the GMPE. However, we assume that ground motion records were captured at two recording stations in proximity to the event. These recordings are used to condition the ground motion fields. Hence, a subset of ground motion fields are selected, which match the recorded IM at the recording sites. The median IM and logarithmic standard deviations for this updated set of ground motion fields are computed.

Fragility curve can then be fit to the updated expected IM. In addition, each point is weighted according to the remaining uncertainty in IM. Weights used are inversely proportional to the logarithmic variance of the simulated IMs for each site (further weight can be added by taking the square of the logarithmic variance). This has the effect of putting larger weights on data in proximity to the recording stations.

The plot in the succeeding text shows the lognormal CDF-based fragility curve fit by MLE with the original IM estimates, the updated IMs, and the updated IMs with weights inversely proportional to the IM variance. The color of the points describes the variance of the IM.

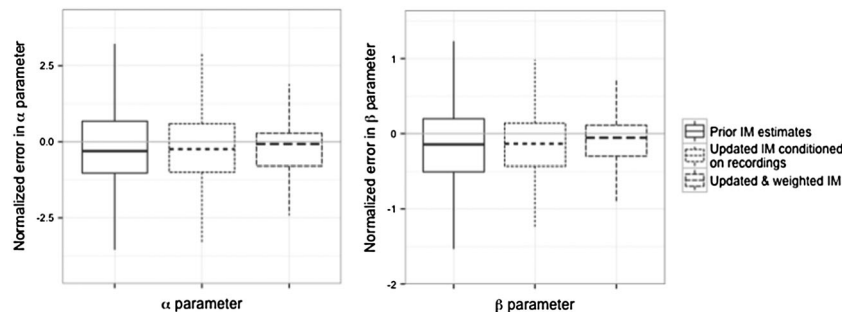


Figure 7. Boxplots of normalized error in parameter estimates of fragility curve due to uncertainty in the intensity measure.

Figure 6 demonstrates the process of updating empirical fragility curves by conditioning the ground motion intensity fields to recordings. However, the ‘true’ fragility curve is still unknown. In order to demonstrate the performance of this procedure, we simulate artificial ‘true’ damage to the Haiti portfolio. A single ground motion field is selected as the true ground motion field experienced. The damage is then simulated for this exposure based on a ‘known’ fragility curve. This simulated damage is then used to fit fragility curves as described earlier and conditioning the ground motion at two arbitrary locations where the intensity matches that of the ‘true’ ground motion intensity field. We use a parametric fragility curve of the lognormal CDF form, using the probit GLM model described in Section 3. This allows for easy comparison of true versus estimated fragility curve parameters. Because damage is artificially generated, any deviation in the fragility curve parameter estimated is due to the uncertainty in the IM.

The process described earlier is repeated iteratively, selecting randomly the ‘true’ ground motion intensity fields, random parameters for the ‘true’ fragility curve, and random pairs of locations for conditioning the IM. The statistics for 2500 such iterations are described in Figure 7.

As observed in Figure 7, the uncertainty in IM results in uncertainty in the parameter estimates of the fragility curve from the empirical damage data. In particular, and as described previously, the uncertainty in IM biases the estimators, which are easily observable from the boxplots of Figure 7. Conditioning the ground motion intensity fields and weighting the IMs based on their variance significantly reduce this bias (to near zero bias), as well as the variability in parameter estimate error. The use of updated median IM and data weighted according to IM variance is easily replicated for all fragility curve fitting methods presented in this paper.

9. SELECTION OF A FRAGILITY FITTING MODEL

The methods described in this paper each result in different fragility curves. The MM and least-squared error methods for fitting the lognormal CDF model are not recommended, because the former merely matches the central moments of the distribution, and the latter assumes Gaussian error and constant variance independent of response, which is inconsistent with the data. All other methods presented have no theoretical reason for disqualification for fitting earthquake fragility. An approach for selection among these methods is therefore necessary.

9.1. Minimum Akaike information criterion (AIC)

There may be good reasons to select only among the parametric models described (MLE-based lognormal CDF, GLMs, and cumulative link models). They have the advantage of simplicity (entire curve summarized in two parameters) and simple inter-comparability. Their parametric form has convenient properties matching requirements of earthquake damage: non-negativity (i.e., no negative IM), monotonic increasing (i.e., higher probability of damage at higher IM), bounded between zero and one (i.e., probability of damage is similarly bounded). Finally, their parameters can be modified, as is commonly done for instance in order to account for additional sources of uncertainty [22, 23].

A common approach for model selection among parametric models is based on their AIC. The AIC measures the goodness of fit while penalizing for model complexity [45]. It is calculated as follows:

$$AIC = -2\log(\text{likelihood}) + 2k \quad (13)$$

where k is the number of parameters in the model, and the *likelihood* is the probability of observing the data given the model. The model with the smallest AIC is the best model. Given that all models considered here have the same number of parameters, an AIC-based selection reduces to select the model with the highest likelihood. Because all the parametric models proposed use MLE as their optimization method, the *likelihood* (and hence, the AIC) is a product of the fitting procedure and is therefore readily extracted from any software package used for fitting.

However, there may be good reasons to opt instead for a non-parametric model or at least compare the predictive power of the parametric and non-parametric models. Non-parametric models have the

Table II. Advantages and disadvantages of various models for fitting fragility curves to empirical or analytical data.

	Advantages	Disadvantages
Lognormal CDF-based curve fit by method-of-moments (MM)	Very simple to implement given appropriate data.	Parametric functions constrain the shape of fragility curves. Can only be used for limited data types (full scale IDA). Provides fit to central values of the sample but not necessarily to the full distribution.
Lognormal CDF-based curve fit by sum of squared error (SSE)	Easily implemented for various data types, including empirical data and analytical data.	SSE method assumes normally distributed error with independent variance, which can result in bias, particularly at low IMs. Parametric functions constrain the shape of fragility curves.
Lognormal CDF-based curve fit by maximum likelihood estimation (MLE) or probit GLM and log(IM)	Lognormal CDF curves generally provide good representations of earthquake damage fragility. Iteratively re-weighted least squares algorithm used for MLE enables non-independent error variance. Easily implemented for various data types, including empirical data and analytical data.	Parametric functions constrain the shape of fragility curves.
Logistic GLM and log(IM)	Commonly used statistical method for dichotomous data. Regression coefficients are estimated using MLE assuming non-independent error variance. Results easy to interpret, as they provide the increase in odds of the response (e.g., odds of collapse) due to a unit increase in input variable (e.g., log(IM)).	Parametric functions constrain the shape of fragility curves.
Cumulative link models	Commonly used statistical method for ordinal data. Ensure proper ordering among cumulative probabilities (no crossing fragility curves) Use all data to fit curves to each damage state, a particular advantage when there is sparse data for a particular damage states (typically, the case for extreme damage or collapse).	Parametric functions constrain the shape of fragility curves. The common effect β shared by fragility curves at different damage states further constrains the flexibility of fragility curves.
Generalized additive models	Commonly used statistical method for dichotomous data. Allow for flexibility and deviation from parametric curves. Can provide very good fit to data.	Can be prone to 'over-fitting', because the resulting curve has less strict functional constraints. Non-parametric curves are more difficult to generalize and interpret.
Gaussian kernel smoothing	Makes no assumption on the distribution of the response and is therefore most true to data observations. Can provide very good fit depending on the data.	Can be prone to 'over-fitting', because the resulting curve has no functional constraints. Non-parametric curves are more difficult to generalize and interpret. May necessitate correction of localized bias at the boundaries.

IDA, Incremental Dynamic Analysis.

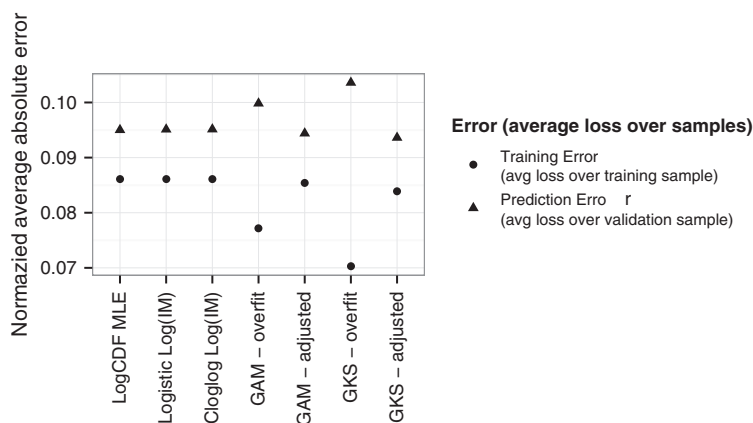


Figure 8. Cross-validation results for fragility models fit to Haiti data.

advantage of being more flexible. In the case of kernel smoothing, no assumptions are made as to the functional form of the data, and it is therefore more ‘true to the observed data’.

The use of AIC as criterion for model selection is not always possible for non-parametric models. The goodness of fit (or likelihood) for the non-parametric models can be arbitrarily good by using more knots in the GAM model (more splines to characterize the curve) or using a smaller bandwidth in GKS. However, computing AIC requires a penalization term related to the number of parameters. For non-parametric models, computing AIC requires estimating the effective number of parameters, which is often impractical.

Cross-validation can be used for model selection of both parametric and non-parametric models. It can also be used to select the smoothing parameters in GAM and GKS models, addressing common issues of over-fitting.

9.2. Cross-validation

Cross-validation is a very common method for estimating expected out-of-sample error. The basic process is to iteratively fit a model on a training sample and measure error against a separate validation sample. By splitting the sample iteratively into training and validation sets, the full distribution of prediction error is obtained.

We first define a loss function. The loss function for error between the true response Y and the prediction model $\hat{f}(IM)$ is denoted $L(Y, \hat{f}(IM))$. Typical loss functions measure the SSE $L(Y, \hat{f}(IM)) = \sum_{i=1} (Y_i - \hat{f}(IM_i))^2$ or the sum of absolute errors $L(Y, \hat{f}(IM)) = \sum_{i=1} |Y_i - \hat{f}(IM_i)|$.

For earthquake damage prediction, the squared error has little meaning, whereas the absolute error directly propagates to errors in loss prediction, fatality prediction, and so on. Hence, the sum of absolute error loss function will be used. Depending on the specific study, other loss functions could be used. For instance, for IDA curves with evenly spaced IMs, a loss function can be developed for measuring the error in annual rate of collapse, after integration with the hazard curve $L(Y, \hat{f}(IM)) =$

$\sum_{i=1} [|Y_i - \hat{f}(IM_i)|\lambda(IM_i)]$, where $\lambda(IM_i)$ is the rate of IM_i . This would have the effect to add more weight to error at the IMs, which most contribute to collapse.

The data are then split into K equal-sized samples (typically 5 or 10 samples). For the k^{th} sample, we fit the model to the remaining data (all but the k^{th} part) and calculate prediction error on the k^{th} sample. This is done iteratively for every k sample and the cross-validation error computed as the average prediction error

$$CV_{err}(\hat{f}) = \frac{1}{K} \sum_{i=1}^K L(Y, \hat{f}^{-k_i}(IM_{ki})) \tag{14}$$

where $\hat{f}^{-k_i}(IM_{k_i})$ is the fragility prediction for IM data in the k_i^{th} samples based on the model fit to the data with the k_i^{th} sample removed.

This same approach can be used to select the appropriate smoothing and bandwidth parameters that minimized cross-validation error, respectively, for GAM and GKS models. The optimal smoothing parameter λ minimizes the cross-validation error as shown in Equation 15.

$$\lambda = \arg \min_{\lambda} [L(Y, \hat{f}(IM, \lambda))] = \min_{\lambda} \sum_{i=1} |Y_i - \hat{f}(IM_i, \lambda)| \quad (15)$$

In this example, the adjusted GKS model displays the least prediction error and is therefore the ‘best’ model because it has the most predictive power. The training error for the overfitted GAM and GKS models is very low. Indeed, they fit the data very well but have much less predictive power on new samples, as is shown from their high prediction error. This is the main advantage of cross-validation, as it provides the out-of-sample error.

Table II provides the general descriptions of the advantages and disadvantages of each method. Cross-validation is a powerful method for evaluating fragility model performance. The results will depend on the specific data used, as well as the loss function for quantifying prediction error. Therefore, the performance of the various models shown in Figure 8 is not absolute, but the process can be repeated for new data or loss function.

10. SUMMARY AND CONCLUSIONS

This paper describes various methods for developing earthquake damage to ground motion intensity relationships. It discusses the commonly used MM and least-squared approaches to fitting lognormal CDF fragility curves, pointing to some of the fundamental flaws with such methods. Instead, equally simple parametric models can be fit with GLMs, which rely on MLE, proper assumptions of binomially distributed data and non-constant error variance. Cumulative link models are used to develop fragility curves for all damage states simultaneously. Taking advantage of the ordinality of damage states, they ensure the proper treatment of cumulative distributions, so that no two fragility curves can cross. They further make use of all damage data for each fragility curves, which are a significant advantage when there are few observations of some damage states. Finally, semi-parametric GAM and non-parametric kernel-based regression are described. These provide significantly more flexibility to fragility models, with the possible danger of overfitting the data. Therefore, cross-validation is used to select smoothing parameters that minimize prediction error. Furthermore, cross-validation is an easily implementable and rigorous method for selecting among competing models based on a user-defined loss criterion.

When developing empirical fragility curves from observed damage data, it is unusual to have actual ground motion recordings at all sites of interest. More commonly, the intensity measures are inferred from GMPEs, combined with few recordings. This leads to issues when fitting a regression model with uncertain independent variable. The paper discusses some of the main challenges with using typical measurement–error models to address this uncertainty, because GMPE-based IM inferences violate many of their fundamental assumptions. However, if even just a few ground motion recordings are available, spatially correlated ground motion intensity fields can be conditioned on such recordings. Given enough ground motion fields, conditional median and standard deviations of IM can be computed at each site. Fragility curves can then be fit to updated IM and each data point weighted inversely to its uncertainty. This simultaneously fits the fragility curve to better predictions and adds more weight to those predictions with least uncertainty (near recording stations).

ACKNOWLEDGEMENTS

The material presented in this paper was developed in part for the Global Earthquake Model foundation (GEM). The partial support provided by GEM is gratefully acknowledged. The research was partially supported by the National Science Foundation Grant NSF CMMI – 106756 by the Shah Family Fellowship and the John A. Blume Fellowship. Discussions with various members of the GEM vulnerability consortium, in

particular Dr. Tiziana Rossetto and Dr. Ioanna Ioannou, were very valuable, and the authors express their appreciation for their comments and input.

REFERENCE

1. Colombi M, Borzi B, Crowley H, Onida M, Meroni F, Pinho R. *Bulletin of Earthquake Engineering* (6th edn). Deriving vulnerability curves using Italian earthquake damage data. Springer: Netherlands, 2008; 485–504. DOI: 10.1007/s10518-008-9073-6
2. Lantada N, Irizarry J, Barbat AH, Goula X, Roca A, Susagna T, Pujades LG. Seismic hazard and risk scenarios for Barcelona, Spain, using the Risk-UE vulnerability index method. *Bulletin of Earthquake Engineering* 2009; **8**: 201–229. DOI: 10.1007/s10518-009-9148-z
3. Braga F, Dolce M, Liberatore D. A statistical study on Damaged Buildings in the 23.11.1980 earthquake, and an ensuing review of the MSK76 scale. Proc 7 European Conference on Earthquake Engineering, 1982.
4. Sabetta F, Goretti A, Lucantoni A. Empirical Fragility Curves from Damage Surveys and Estimated Strong Ground Motion. Proceedings of the 11th European Conference on Earthquake Engineering, 1998.
5. Singhal A, Kiremidjian AS. Method for probabilistic evaluation of seismic structural damage. *Journal of Structural Engineering* 1996; **122**: 1459–1467. DOI:10.1061/(ASCE)0733-9445(1996)122:12(1459)
6. Rossetto T, Elnashai A. A new analytical procedure for the derivation of displacement-based vulnerability curves for populations of RC structures. *Engineering Structures* 2005; **27**: 397–409. DOI: 10.1016/j.engstruct.2004.11.002
7. Ibarra LF, Krawinkler H. Global collapse of frame structures under seismic excitations. Blume Center Technical Report, 2005.
8. Federal Emergency Management Agency (FEMA). HAZUS Earthquake Loss Estimation Methodology. US Federal Emergency Management Agency, 1999.
9. Jaiswal, KS, Aspinall W, Perkins D. Use of Expert Judgment Elicitation to Estimate Seismic Vulnerability of Selected Building Types. Proc 15th World Conference on Earthquake Engineering, 2012; 1–10.
10. Applied Technology Council. Earthquake damage evaluation data for California (ATC-13). *Applied Technology Council*. Redwood City, CA, 1985.
11. Ministère des Travaux Publics, Transports et Communications, 2013. <http://www.mtptc.gouv.ht>.
12. Boore DM, Atkinson GM. Ground-motion prediction equations for the average horizontal component of PGA, PGV, and 5%-damped PSA at spectral periods between 0.01 s and 10.0 s. *Earthquake Spectra* 2008; **24**: 99–138. DOI: 10.1193/1.2830434
13. Hayes G. Finite Fault Model: Updated Result of the Jan 12, 2010 Mw 7.0 Haiti Earthquake. National Earthquake Information Center (NEIC) of United States Geological Survey, 2014.
14. Vamvatsikos D, Allin Cornell C. Incremental dynamic analysis. *Earthquake Engineering & Structural Dynamics* 2002; **31**: 491–514. DOI: 10.1002/eqe.141
15. Mazzoni S, McKenna F, Scott MH, Fenves GL. Open System for Earthquake Engineering Simulation (OpenSees). *Pacific Earthquake Engineering Research Center* 2006.
16. Federal Emergency Management Agency. Quantification of building seismic performance factors (FEMA P695), 2009.
17. Burton H, Deierlein GG. Simulation of seismic collapse in non-ductile reinforced concrete frame buildings with masonry infills. *Journal of Structural Engineering* 2014; **140**(8): A4014016.
18. Bradley BA, Dhakal RP. Error estimation of closed-form solution for annual rate of structural collapse. *Earthquake Engineering & Structural Dynamics* 2008; **37**: 1721–1737. DOI: 10.1002/eqe.833
19. Sarabandi P, Pachakis D, King S. Empirical fragility functions from recent earthquakes. 13th World Conference on Earthquake Engineering, 2004.
20. Bird JF, Bommer JJ, Bray JD, Sancio R, Spence RJS. Comparing loss estimation with observed damage in a zone of ground failure: a study of the 1999 Kocaeli Earthquake in Turkey. *Bulletin of Earthquake Engineering* 2004; **2**: 329–360. DOI: 10.1007/s10518-004-3804-0
21. Kennedy RP, Cornell CA, Campbell RD, Kaplan S, Perla HF. Probabilistic seismic safety study of an existing nuclear power plant. *Nuclear Engineering and Design* 1980; **59**: 315–338. DOI: 10.1016/0029-5493(80)90203-4
22. Kennedy RP, Ravindra MK. Seismic fragilities for nuclear power plant risk studies. *Nuclear Engineering and Design* 1984; **79**: 47–68. DOI: 10.1016/0029-5493(84)90188-2
23. Kircher CA, Aladdin A, Nassar OK, Holmes WT. Development of building damage functions for earthquake loss estimation. *Earthquake Spectra* 1997; **13**: 663–682. DOI: 10.1193/1.1585974
24. Shinozuka M, Feng MQ, Lee J, Naganuma T. Statistical analysis of fragility curves. *Journal of Engineering Mechanics* 2000; **126**: 1224–1231. DOI: 10.1061/(ASCE)0733-9399(2000)126:12(1224)
25. US Nuclear Regulatory Commission. *PRA Procedures Guide: A Guide to the Performance of Probabilistic Risk Assessments for Nuclear Power Plants (NUREG-2300)*. Office of Nuclear Regulatory Research: Washington, DC, 1983.
26. Porter K, Kennedy R, Bachman R. Creating fragility functions for performance-based earthquake engineering. *Earthquake Spectra* 2007; **23**: 471–489. DOI: 10.1193/1.2720892
27. Baker JW. Efficient analytical fragility function fitting using dynamic structural analysis. *Earthquake Spectra*, p.141208072728004, 2014.
28. Rota M, Penna A, Strobbia CL. Processing Italian damage data to derive typological fragility curves. *Soil Dynamics and Earthquake Engineering* 2008; **28**: 933–947. DOI: 10.1016/j.soildyn.2007.10.010
29. Straub D, Der Kiureghian A. Improved seismic fragility modeling from empirical data. *Structural Safety* 2008; **30**: 320–336. DOI: 10.1016/j.strusafe.2007.05.004

30. McCullagh P, Nelder JA. *Generalized Linear Model* (2nd edn). Chapman & Hall/CRC: Boca Raton, Florida, 1989. ISBN 0-412-31760-5
31. Agresti A. *Categorical Data Analysis*. Wiley-Interscience: New York, NY, 2002.
32. Basöz NI, Kiremidjian AS. *Evaluation of Bridge Damage Data from the Loma Prieta and Northridge, California Earthquakes*. Technical Report MCEER. U.S. Multidisciplinary Center for Earthquake Engineering Research, 1998.
33. O'Rourke MJ, So P. Seismic fragility curves for on-grade steel tanks. *Earthquake Spectra* 2000; **16**: 801–815. DOI: 10.1193/1.1586140
34. Wood SN. On confidence intervals for generalized additive models based on penalized regression splines. *Australian & New Zealand Journal of Statistics* 2006; **48**: 445–464. DOI: 10.1111/j.1467-842X.2006.00450.x
35. Hastie T, Tibshirani J, Jerome J, Friedman H. *The Elements of Statistical Learning: Data Mining, Inference, and Prediction* (2nd edn). Springer, 2009. ISBN-13: 978-0387952840
36. Rossetto T, Ioannou I, Grant DN, Maqsood T. GEM guidelines for empirical vulnerability assessment. *Global Earthquake Model report* 2014; 1–108. <http://www.nexus.globalquakemodel.org/gem-vulnerability/posts/guidelines-for-empirical-vulnerability-assessment> (Accessed June 2014).
37. Noh HY, Lignos DG, Nair KK. Development of fragility functions as a damage classification/prediction method for steel moment-resisting frames using a wavelet-based damage sensitive feature. *Earthquake Engineering & Structural Dynamics* 2011. DOI: 10.1002/eqe.1151
38. Noh HY, Lallemand D, Kiremidjian A. Development of empirical and analytical fragility functions using kernel smoothing methods. *Earthquake Engineering & Structural Dynamics* 2014. DOI: 10.1002/eqe.2505
39. Applied Technology Council. *Seismic Performance Assessment of Buildings - Volume 1 - Methodology*. Applied Technology Council: Redwood City, CA, 2012.
40. Singhal A, Kiremidjian AS. Bayesian updating of fragilities with application to RC frames. *Journal of Structural Engineering* 1998; **124**: 922–929. DOI: 10.1061/(ASCE)0733-9445(1998)124:8(922)
41. Gardoni P, Der Kiureghian A, Mosalam KM. Probabilistic capacity models and fragility estimates for reinforced concrete columns based on experimental observations. *Journal of Engineering Mechanics* 2002; **128**: 1024–1038. DOI: 10.1061/(ASCE)0733-9399(2002)128:10(1024)
42. Jaiswal K, Wald D, D'Ayala D. Developing empirical collapse fragility functions for global building types. *Earthquake Spectra* 2011; **27**: 775–795. DOI: 10.1193/1.3606398
43. Fuller WA. *Error Measurement Models*. John Wiley: New York, 1987.
44. Jayaram N, Baker J. *Correlation Model for Spatially Distributed Ground-Motion Intensities*. *Earthquake Engineering & Structural Dynamics* 2009. DOI: 10.1002/eqe.922
45. Akaike H. A new look at the statistical model identification. *Automatic Control, IEEE Transactions on IEEE* 1974; **19**: 716–723. DOI: 10.1109/TAC.1974.1100705